Electronic Supplementary Material (ESI) for Dalton Transactions

Supporting Information

Spin crossover and polymorphism in a family of 1,2-bis(4-pyridyl)ethene-bridged binuclear iron(II) complexes. A key role of structural distortions.

G. S. Matouzenko,* E. Jeanneau, A. Yu. Verat, and A. Bousseksou

Table S1. Crystallographic Data for **1, 2, and 3**[a]

	1	**1**	**1**	**2**	**3**
Spin state	HS–HS	HS–LS	LS–LS	HS–HS	HS–HS
Formula	$C_{40}H_{36}N_{12}S_4Fe_2$	$C_{40}H_{36}N_{12}S_4Fe_2$	$C_{40}H_{36}N_{12}S_4Fe_2$	$C_{42}H_{44}N_{12}S_4O_2Fe_2$	$C_{40}H_{36}N_{12}S_4Fe_2$
M	924.79	924.79	924.79	988.87	924.79
T [K]	300	183	90	290	293
Crystal system	monoclinic	monoclinic	monoclinic	monoclinic	monoclinic
Space group	$C2/c$	$C2/c$	$C2/c$	$P2_1/n$	$P2_1/c$
a/Å	20.813(1)	21.017(3)	20.759(1)	10.305(1)	17.092(5)
b/Å	12.745(1)	12.429(1)	12.249(1)	16.467(2)	16.804(5)
c/Å	18.935(1)	19.390(3)	19.400(1)	14.043(1)	16.316(5)
β/°	111.389(2)	114.08(2)	114.008(2)	96.61(1)	106.911(5)
V/Å^3	4676.8(3)	4624.3(1)	4506.2(3)	2367.1(4)	4484(2)
ρ_{calcd}/g cm^3	1.313	1.328	1.363	1.387	1.371
Z	4	4	4	2	4
λ/Å	0.71069	0.71069	0.71069	0.71069	0.71069
$\mu(Mo_{K_\alpha})$/mm^{-1}	0.840	0.850	0.872	0.838	0.877
F(000)	1904	1904	1904	1024	1904
θ range/°	1.9–27.9	3.3–29.5	2.0–27.9	3.6–29.6	2.9–29.3
independent reflections	5097	5693	5252	5911	10295
independent reflections with $I>2\sigma(I)$	2823	3574	4197	3130	3229
parameters	280	262	262	280	523
$R[F^2>2\sigma(F)^2]$	0.0681	0.0670	0.0735	0.0527	0.0843
$wR_2(F^2)$	0.1687	0.0880	0.1964	0.1386	0.1837

[a]Estimated standard deviations in the least significant digits are given in parentheses.

Table S2. Selected Bond Distances (Å) and Angles (deg) for **1, 2, and 3**[a]

	1	**1**	**1**	**2**	**3** (Fe1 site)[b]	**3** (Fe2 site)[c]
	300 K	183 K	90 K	290 K	293 K	293 K
Fe(1)-N(1)	2.108(5)	2.014(4)	1.952(3)	2.111(4)	2.085(9)	2.106(10)
Fe(1)-N(2)	2.089(5)	1.991(4)	1.954(3)	2.093(5)	2.095(10)	2.129(9)
Fe(1)-N(3)	2.199(4)	2.073(4)	1.992(3)	2.208(4)	2.196(10)	2.202(10)
Fe(1)-N(4)	2.248(4)	2.114(3)	2.017(3)	2.239(4)	2.216(9)	2.201(10)
Fe(1)-N(5)	2.222(4)	2.075(3)	1.967(3)	2.163(4)	2.289(9)	2.198(10)
Fe(1)-N(6)	2.202(4)	2.081(3)	1.997(3)	2.219(4)	2.218(9)	2.220(9)
N(1)-Fe(1)-N(2)	95.8(2)	93.1(2)	90.6(1)	96.8(2)	101.7(5)	100.6(4)
N(1)-Fe(1)-N(3)	94.7(2)	94.0(2)	93.3(1)	94.9(2)	93.4(4)	92.8(4)
N(1)-Fe(1)-N(4)	166.1(2)	171.8(2)	175.4(1)	168.5(2)	158.1(4)	165.8(4)
N(1)-Fe(1)-N(5)	92.9(2)	93.8(1)	94.1(1)	96.6(2)	90.5(4)	94.2(4)
N(1)-Fe(1)-N(6)	96.7(2)	94.3(2)	92.0(1)	91.8(2)	97.7(4)	91.1(4)
N(2)-Fe(1)-N(3)	101.8(2)	97.7(1)	95.1(1)	93.3(2)	85.5(4)	94.0(4)
N(2)-Fe(1)-N(4)	96.2(2)	93.0(2)	91.6(1)	89.4(2)	96.6(4)	89.4(4)
N(2)-Fe(1)-N(5)	169.0(2)	172.0(1)	174.6(1)	166.6(2)	166.3(4)	164.7(4)
N(2)-Fe(1)-N(6)	87.9(2)	87.4(1)	87.4(1)	89.3(2)	86.9(4)	85.9(4)
N(3)-Fe(1)-N(4)	75.9(2)	79.7(1)	82.4(1)	75.1(2)	76.2(4)	76.3(4)
N(3)-Fe(1)-N(5)	84.1(2)	85.9(1)	87.3(1)	85.2(1)	100.0(3)	89.0(3)
N(3)-Fe(1)-N(6)	164.2(2)	170.0(1)	174.1(1)	172.5(2)	167.7(4)	176.0(4)
N(4)-Fe(1)-N(5)	76.1(2)	80.5(1)	83.9(1)	77.3(2)	72.9(3)	76.8(4)
N(4)-Fe(1)-N(6)	90.8(2)	91.5(1)	92.2(1)	98.0(2)	95.1(4)	99.7(4)
N(5)-Fe(1)-N(6)	84.4(2)	88.1(1)	89.7(1)	90.7(1)	85.4(3)	90.1(4)

[a] Estimated standard deviations in the least significant digits are given in parentheses
[b] N(1), N(2), N(3), N(4), N(5), and N(6) correspond to N(101), N(102), N(103), N(104), N(105), and N(106), respectively
[c] N(1), N(2), N(3), N(4), N(5), and N(6) correspond to N(201), N(202), N(203), N(204), N(205), and N(206), respectively

Table S3. Least-squares-fitted Mössbauer data[a]

T (K)	δ (mms^{-1})	$\Gamma/2$ (mms^{-1})	ΔE_q (mms^{-1})	δ (mms^{-1})	$\Gamma/2$ (mms^{-1})	ΔE_q (mms^{-1})	A_{HS}/A_{tot}
	[HS–HS]			[LS–LS]			
293	1.013(2)	0.159(4)	1.625(5)	0.43	0.6(2)	0.22	0.95(3)
220	1.069(4)	0.231(5)	1.89(7)	0.458(3)	0.204(6)	0.16(2)	0.57(2)
200	1.086(5)	0.301(7)	1.984(9)	0.455(3)	0.225(5)	0.253(6)	0.452(9)
150	1.146(6)	0.245(9)	2.23(2)	0.455(3)	0.225(5)	0.253(6)	0.151(6)
80	1.07(2)	0.16(2)	2.68(3)	0.490(5)	0.186(2)	0.196(2)	0.032(3)

[a] δ : isomer shift (with reference to metallic iron at 293 K), ΔE_q: quadrupole splitting, Γ: half-height width, A_{HS} : area of HS doublet, A_{tot} : total Mössbauer spectrum area. The error bars of statistical origin are given in parentheses. Values without error bars have been fixed for the fit.

Table S4. Calculated Bond Distances (Å) and Angles (deg) for the HS site in the [HS–LS] pairs

	$[\{Fe(dpia)(NCS)_2\}_2(bpy)]$	$[\{Fe(bt)(NCS)_2\}_2bpym]$	$\{[(Fe(bztpen)]_2[N(CN)_2]\}(PF_6)_3$ Fe1 site	$\{[(Fe(bztpen)]_2[N(CN)_2]\}(PF_6)_3$ Fe2 site
Fe(1)-N(1)	2.069	2.171	2.131	2.120
Fe(1)-N(2)	2.046	2.211	2.128	2.128
Fe(1)-N(3)	2.174	2.237	2.204	2.173
Fe(1)-N(4)	2.226	2.201	2.204	2.228
Fe(1)-N(5)	2.191	2.075	2.218	2.225
Fe(1)-N(6)	2.198	2.027	2.048	2.055
N(1)-Fe(1)-N(2)	97.7	73.8	91.3	91.1
N(1)-Fe(1)-N(3)	92.1	94.6	168.2	167.7
N(1)-Fe(1)-N(4)	165.8	157.8	95.2	96.3
N(1)-Fe(1)-N(5)	93.6	95.8	79.7	78.9
N(1)-Fe(1)-N(6)	93.8	98.7	95.5	95.9
N(2)-Fe(1)-N(3)	97.3	84.4	91.4	91.0
N(2)-Fe(1)-N(4)	93.0	86.0	155.0	155.0
N(2)-Fe(1)-N(5)	168.2	164.8	76.4	76.3
N(2)-Fe(1)-N(6)	90.7	95.2	105.7	106.7
N(3)-Fe(1)-N(4)	77.5	74.1	78.2	77.7

Electronic Supplementary Material (ESI) for Dalton Transactions

Figure S1. Stick representation of **1** showing a twist of the bridging bpe ligand.

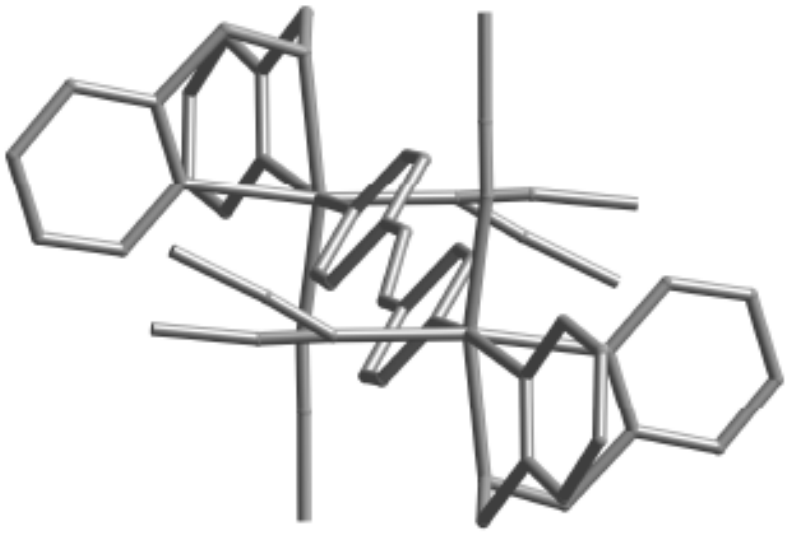

Figure S2. Representation of the two modes of π stacking interactions at 300 K.

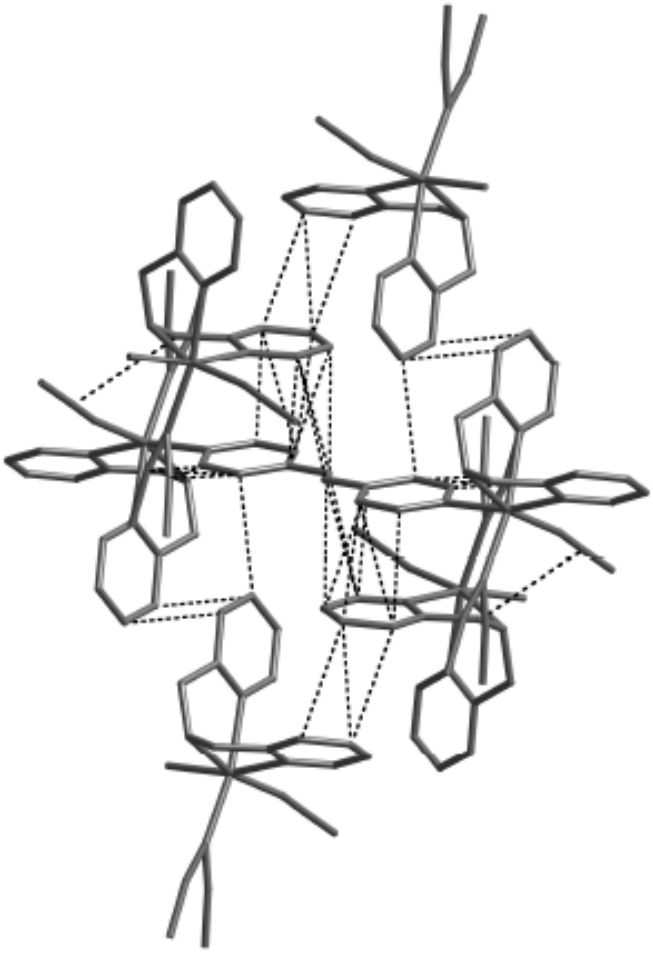

Figure S3. Projection of the structure of **2** on the *ab* plane showing the hydrogen bonding with the corresponding atom-numbering scheme.